Structural and electrical-physical properties of the ohmic contacts based on palladium to n^+-n-n^{++}-n^{+++}-InP

A.E. Belyaev[1], N.A. Boltovets[2], A.B. Bobyl[3], V.P. Kladko[1], R.V. Konakova[1], Ya.Ya. Kudryk[1], M.U. Nasyrov[1], A.V. Sachenko[1], V.S. Slipokurov[1], A.S. Slepova[2], N.V. Safryuk[1], A.I. Gudymenko[1], V.V. Shynkarenko[1]

[1]*V. Lashkaryov Institute of Semiconductor Physics, National Academy of Sciences of Ukraine*
41, prospect Nauky, 03680 Kyiv, Ukraine, e-mail: konakova@isp.kiev.ua
[2]*State Enterprise Research Institute "Orion", 03057 Kyiv, Ukraine*
[3]*A.F. Ioffe Physical-Technical Institute, Russian Academy of Sciences,*
197101, St. Petersburg, Russian Federation

Abstract. Presented in this paper are experimental data on structural properties of contact metallization and temperature dependence of the specific contact resistance for ohmic contacts Au–Ti–Pd–n^+-InP and Au–Ti–Ge–Pd-n^+-InP prepared using the method of successive thermal evaporation of metals in oil-free vacuum in one process cycle onto the n^+-n-n^{++}-n^{+++}-InP epitaxial structure heated to 300 °C. It has been theoretically and experimentally shown that within the temperature range 250…380 K the current transport mechanism in the ohmic contacts Au–Ti–Pd–n^+-InP is thermal-field one, and in the ohmic contacts Au–Ti–Ge–Pd-n^+-InP it is caused by conductivity along metal shunts linked with dislocations. According to the X-ray diffraction data, the density of these dislocations in the near-contact InP area is ~10^9 cm^{-2}.

Keywords: ohmic contacts, specific contact resistance, InP, current transport mechanism.

1. Introduction

Indium phosphide is one of the main semiconductor materials currently used for manufacturing Gunn diodes and field-effect transistors with high mobility – high-electron mobility transistor (HEMT) of millimeter and submillimeter wavelengths [1-4]. These devices are characterized with very small dimensions. Therefore, it is natural to demand high structural homogeneity to forming contact layers and the interface metal-InP. This requirement applies equally to both rectifying (barrier) and nonrectifying (ohmic) contacts. For ohmic contacts to the indium phosphide microwave devices, gold-germanium eutectic is most often used.

For all the merits of such contact (it is known since the first experiments on GaAs Gunn diode [5]), the presence of interfacial interactions, which are accompanied by formation of a number of new phases that originate in the process of formation of ohmic contacts and possible overloads in the operation of devices in electronic sets, causes significant heterogeneity of the interface 'forming contact layer – InP'. In this case, the phases originating at relatively low temperatures do not break down at higher ones, too [6]. It leads to a non-uniform distribution of the current density over the contact area. In addition, the heterogeneity in the height of the barrier arises [7]. I.e., the layered structure not only of contact metallization,

but the area of the interface 'forming contact layer – InP' is significantly broken. Therefore, still there is a necessity to search for optimizing the parameters of the ohmic contacts to InP and methods of their manufacturing [8-10].

For example, formation of the contact metallization to InP with the first deposited metal layer, contributing to improvement of adhesion. This layer is called as adhesive one having oxidation resistance and relatively low temperature of reaction with InP, which should provide adhesion. Annealing of the contact metallization with the adhesive layer within the temperature range 300 to 450 °C results in formation of an ohmic contact. Thus, when preparing the ohmic contact Pd–n-InP ($n \approx 10^{17}$ cm^{-3}) using electron-beam evaporation, followed by annealing within the temperature range 300…375 °C, a minimum specific contact resistivity of ~4.2·10^{-6} Ohm·cm^2 was obtained [11].

When creating the ohmic contact Au–Ge–Pd–n-InP ($n \approx 10^{17}$ cm^{-3}) by using the same technological process, but with annealing within the temperature range 350…450 °C, the minimum value ρ_c was close to 2.5·10^{-6} Ohm·cm^2 [11]. At the same time, up to date for these contacts a number of important physical and technological parameters have not been studied, including temperature dependences of ρ_c, influence of structural defects that originate during annealing and cooling the samples in the area of the interface 'forming contact layer – InP' due to relaxation of internal mechanical strains on the value ρ_c and dependence $\rho_c(T)$. We also note a particular interest of developers of technology for devices based on A^{3}B^5 compounds to the reduction of the number of heat treatments, which, on the one hand, reduces the cost of production of devices and, on the other hand, improves the quality of the active elements. Currently, non-annealed ohmic contacts are used in the technological process of creation of HEMT based on the compounds A$_3$N [12].

Below, the research of ohmic contacts based on palladium to the epitaxial structure n^+-n-n^{++}-n^{+++}-InP is presented. The ohmic contacts Au–Ti–Pd–n^+-InP and Au–Ti–Ge–Pd–n^+-InP were created to the upper epitaxial n^+-layer InP.

2. Samples and research methods

There were investigated two types of the samples: the test structures for measuring specific contact resistivity ρ_c within the temperature range 250…380 K with the use of transmission line method (TLM) and the test structures with continuous metallization for measuring the profile of distribution of the components as well as phase composition of the contact metallization by the methods of Auger electron spectroscopy and X-ray diffractometry, respectively. The elemental composition was measured using Auger spectrometer LAS-2000, the phase composition and deformation effects – setup ARL X'Tra (Thermo scientific) with CuKα radiation and database ICDD, PDF-2 Release 2012.

Ohmic contacts were formed using the method of successive thermal deposition of metals in oil-free vacuum in a single processing cycle onto heated to 300 °C substrate that is epitaxial structure n^+-n-n^{++}-n^{+++}-InP obtained using gas-phase epitaxy. The structure parameters are the concentration of the donor impurity (Si) in the layers: $n^+ – 10^{18}$ cm^{-3}, $n – 8·10^{15}$ cm^{-3}, $n^{++} – 5·10^{17}$ cm^{-3}, $n^{+++} – 2·10^{18}$ cm^{-3}, the thicknesses of the layers: 0.2, 15, 3, and 300 μm, respectively. The ohmic contacts Au (100 nm)–Ti (40 nm)–Pd (30 nm)–n^+-InP and Au(200 nm)–Ti(40 nm)–Ge(60 nm)–Pd(30 nm)–n^+-InP were formed during the deposition process and not subjected to the additional annealing.

3. Experimental results and discussion

Figs 1 and 2 shows the profiles of distribution of the components in the contact metallization Au–Ti–Pd–n^+-InP and Au–Ti–Ge–Pd–n^+-InP formed on the heated to 300 °C substrates. As seen from these figures, both types of contacts have a layered structure. In both cases, the increased content of oxygen and carbon in the titanium film is observed. For the sample Au–Ti–Ge–Pd–n^+-InP (Fig. 2), typical is the mass transport of Ge into the thin near-contact area of InP, which causes the increase in the concentration of the donor impurity (Ge is the donor in InP [13]) in this area. The peculiarity of the near-contact area of InP in both samples is its multicomponent character, as can be seen from Figs 1 and 2.

The XRD analysis of the test structures with both types of metallization has shown the presence of reflections from the polycrystalline Au and Ti films (Figs 3 and 4) and absence of corresponding reflections from Ge and Pd or their compounds with InP. As Pd and Ge are observed in the corresponding profiles of the contact metallization to n^+-InP (Figs 1 and 2), it can be assumed that during deposition of metal on a heated to 300 °C substrate, the products of the phase formation are created in the amorphous phase. This assumption does not contradict the available data in the literature about the ohmic contacts to InP based on palladium [11, 14].
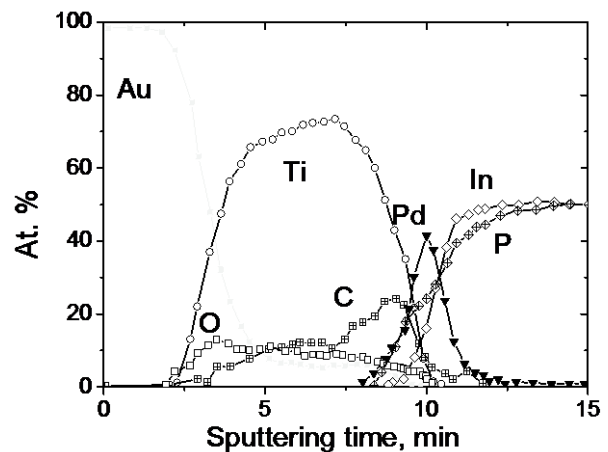

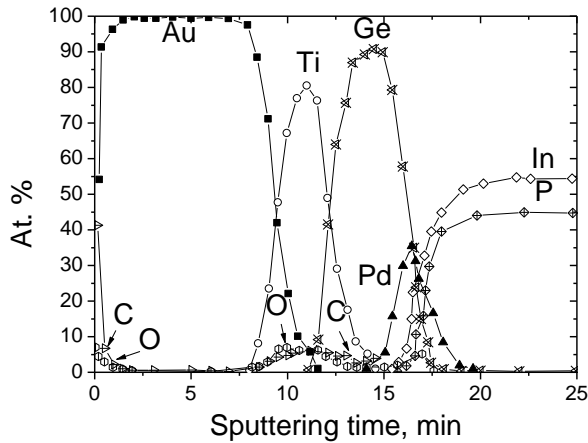**Fig. 1.** Profiles of component distribution in the contact metallization Au–Ti–Pd–n^+-InP.

Fig. 2. Profiles of component distribution in the contact metallization Au–Ti–Ge–Pd–n^+-InP.

The analysis of diffraction spectra indicates the difference in the elastic-strain state of two contact systems. In particular, for the system Au–Ti–Pd–n^+-InP (Fig. 3), the values of deformations in the contact metallization is about 0.014, while for the system Au–Ti–Ge–Pd–n^+-InP (Fig. 4) this value is lower; i.e., the contact Au–Ti–Ge–Pd–n^+-InP is more relaxed [15, 16]. The analysis of the deformation state of the contact systems shows that the main mechanism of relaxation of strains in the system Au–Ti–Ge–Pd–n^+-InP is generation of dislocations in the near-contact area of InP with the density of the order of 10^9 cm^{-2}. It is these defects of this type that are the main cause of the structural heterogeneity in the near-contact area.

The voltage-current characteristics of the contacts Au–Ti–Pd–n^+-InP and Au–Ti–Ge–Pd–n^+-InP within the temperature range 250…380 K were linear. The temperature dependences ρ_c to these contacts measured within the temperature range 250…380 K are shown in Fig. 5. The analysis of the dependences $\rho_c(T)$ showed that for the ohmic contacts Au–Ti–Pd–n^+-InP (empty points in the curve *1*, Fig. 5) thermal-field current transport mechanism is characteristic, for Au–Ti–Ge–Pd–n^+-InP (filled points in the curve 2, Fig. 5) – the current transport mechanism through metal shunts. In what follows, they will be considered in more detail.

Let plot a relationship $\rho_c(T)$ for ohmic contact Au–Ti–Pd–n^+-InP in accordance with the modified formula for the thermal-field current transport mechanism [17]:

$$\rho_{TF} = \frac{k\sqrt{E_{00}}\cosh\left(\dfrac{E_{00}}{kT}\right)\coth\left(\dfrac{E_{00}}{kT}\right)}{A\left(\dfrac{m^*}{m_0}\right)Tq\sqrt{\pi(\varphi_c - E_F)}} \times$$

$$\times \exp\left[\frac{\varphi_c - E_F}{E_{00}\coth\left(\dfrac{E_{00}}{kT}\right)} + \frac{E_F}{kT}\right], \tag{1}$$

where ρ_{TF} is the specific contact resistivity in the case of the thermal-field current transport mechanism, k – Boltzmann constant, T – temperature, q – elementary charge, m^* – effective mass of electron, m_0 – free electron mass, φ_c – potential energy of electron, i.e., the barrier height at the interface metal-semiconductor, $E_{00} = 0.054\left((m_0/m^*)(N_d/10^{20})(11.7/\varepsilon_s)\right)^{0.5}$ – characteristic energy of tunneling, ε_s – dielectric constant of semiconductor, A – the Richardson constant, E_F – the Fermi energy, N_d – donor concentration. Indeed, as can be seen from a comparison of the experimental and theoretical dependences $\rho_c(T)$ (Fig. 5, curve *1*: dots – experiment, line – calculation), they are in good agreement with each other. The coincidence is achieved in the case where the barrier height is 0.28 eV.
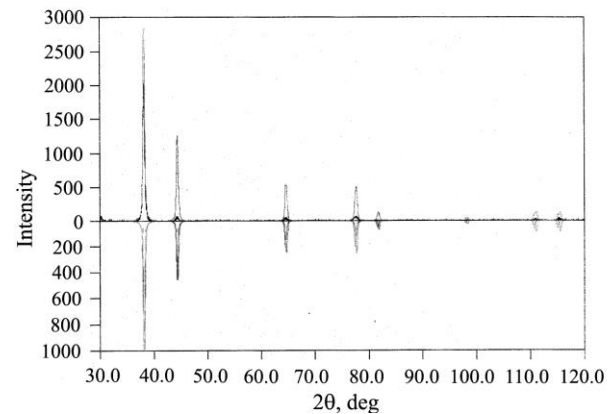

Fig. 3. Experimental diffraction pattern of the contact metallization Au–Ti–Pd–n^+-InP (upper curve) and calculated diffraction patterns for Au and Ti (lower curves).
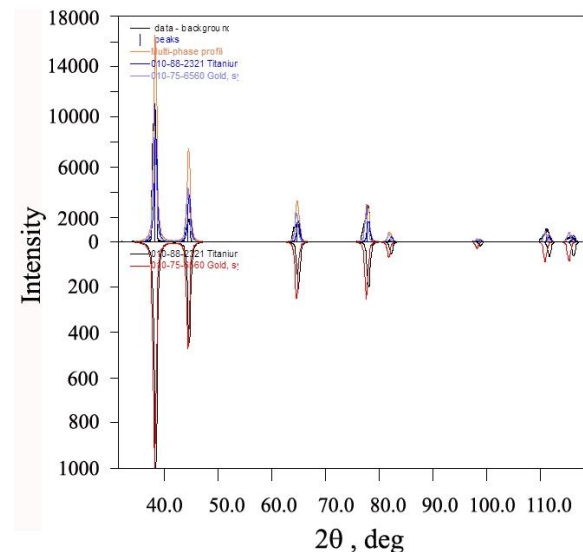

Fig. 4. Experimental diffraction pattern of the contact metallization Au–Ti–Ge–Pd–n^+-InP (upper curves) and calculated diffraction patterns for Au and Ti (lower curves).
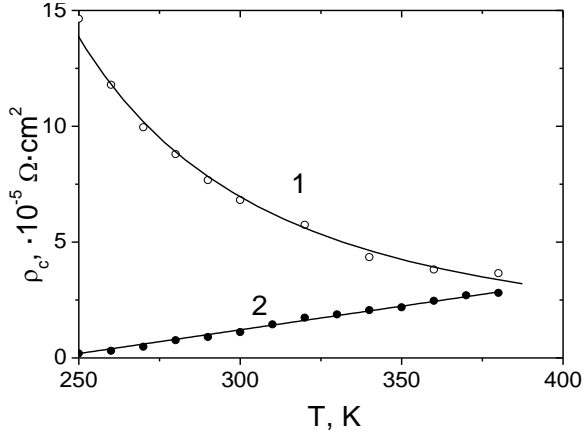
Fig. 5. Temperature dependence of the specific contact resistance (*1* – Au–Ti–Pd–n^+-InP, *2* – Au–Ge–Ti–Pd–n^+-InP, dots – experiment, lines – calculation).

Since the literature data on the dependence $\rho_c(T)$ for ohmic contacts based on Pd are absent, let's compare the ρ_c values measured at room temperature [14] with those obtained in our work. Thus, the ohmic characteristics for contact Pd-InP were observed after annealing at $T = 300$ °C and were caused by the presence of the phase PdIn. For such a contact, the ρ_c value at room temperature was about $6\cdot10^{-5}$ Ohm·cm^2 [14]. ρ_c of the same order was obtained in our work after deposition of metals (Pd, Au and Ti) onto the substrate heated to 300 °C (Fig. 5, curve *1*).

Our data on $\rho_c(T)$ as well as on the phase and chemical composition of the contact metallization of Au–Ti–Pd–n^+-InP indicate relatively uniform interface 'forming contact layer – InP' created directly during deposition of the contact metallization on the InP substrate heated to 300 °C without subsequent heat treatment.

The analysis of the ohmic contacts, in which the composition together with the adhesion layer Pd includes Ge, has shown that at room temperature for different samples and annealing conditions, ρ_c varies within the range $10^{-5}...2.5\cdot10^{-6}$ Ohm·cm^2 according to [14]. In our work (Fig. 5, curve *2*), during deposition of metals (Pd, Ge, Ti, and Au) on the heated to 300 °C substrate, at room temperature ρ_c is close to $1.2\cdot10^{-5}$ Ohm·cm^2. I.e., as in the previous case (contact Au–Ti–Pd–n^+-InP), the ρ_c value is of the same order as those of the samples, in which the ohmic contact has formed after annealing.

In the theoretical simulation of the dependence $\rho_c(T)$ for the ohmic contact Au–Ti–Ge–Pd–n^+-InP, we take into account that in this case the subcontact layer n^+-InP is strongly degenerated due to subdoping with germanium. As seen from Fig. 5 (curve *2*), at $T > 250$ K $\rho_c(T)$ is linearly dependent on the temperature. In accordance with [18], we assume that the current transport occurs through the metal shunts linked with dislocations. To calculate $\rho_c(T)$, we use the expressions [18] valid for the case of degenerated semiconductor.

Following [18], we write an expression for the specific contact resistivity ρ_{tw} that is determined by the supply of electrons from semiconductor into the ends of shunts for the contact of unit area

$$\rho_{tw} = \frac{k}{q\pi N_{D1}L_D^2 A(m^*/m_0)T} \frac{1}{\ln\left[1+\exp\left(z+y_{c0}\right)\right]} , (2)$$

where N_{D1} is the density of conductive dislocations, L_D – Debye screening length, y_{c0} – dimensionless (normalized to kT) contact potential. In the considered case, the dimensionless Fermi energy z (normalized to kT) is determined from the equation of volume neutrality:

$$N_d = \frac{2}{\sqrt{\pi}} N_{c0} \left(\frac{T}{300}\right)^{3/2} \int_0^\infty \frac{x}{1+\exp(x-z)} dx , (3)$$

where N_{c0} is the effective density of states in the conduction band.

It should be noted that the stronger degenerated semiconductor, the weaker the value ρ_{tw} depends on the temperature, and with threshold levels of degeneration when $z + y_{c0} \gg 1$, the dependence ρ_{tw} is absent. Since the resistivity of all the metal shunts ρ_{sh} is connected in series with the resistivity ρ_{tw} in the case of degenerated semiconductor, the relation for the total resistivity of the ohmic contact in semiconductor with a high dislocation density is written as

$$\rho_c = \rho_{tw} + \rho_{sh} . (4)$$

Here, $\rho_{sh} = R_{sh}(T)/N_{D1}$ and $R_{sh}(T) = \frac{\rho_0(T)d_D}{\pi r^2}$

is the temperature dependence of the resistance of metal shunt, where ρ_0 is the specific resistivity, d_D – dislocation length, r – shunt radius (in the calculation, all the shunts are considered to be identical). It is assumed that the current flowing between dislocations can be neglected in comparison with the current flowing through these dislocations. It is provided by the large value of the barrier formed between dislocations [18].

The temperature dependence $\rho_{sh}(T)$ with account of the temperature dependence of the resistivity of forming contact metal at $T > 250$ K is linear, since $T \geq T_D$, where T_D is the Debye temperature, i.e., the metal resistance increases linearly with the temperature: $\rho_0(T) = \rho_{00}(1+\alpha(T-250))$, where α is the temperature coefficient of resistance.

The theoretical curve for the dependence $\rho_c(T)$ was calculated using the formula (4). As can be seen from Fig. 5 (curve *2*, line is calculation, points – experiment), there is a good agreement between the calculated dependence of the specific contact resistivity ρ_c with the experimental data. It is achieved by using the following parameters: $N_{D1} \approx 10^9$ cm^{-2}, $r \approx 6\cdot10^{-8}$ cm, $d_D \sim 0.1$ μm, $\alpha \approx 3\cdot10^{-2}$ K^{-1}. Estimation of the dislocation density obtained from the X-ray diffraction data almost coincides with the N_{D1} value calculated using the formula (4).

Attention is drawn to the fact that in this case the α value is much higher than the temperature coefficient of resistance growth for pure metals. It may be caused by the fact that in this case forming contact layer is a multicomponent alloy.

It has been shown that the ohmic contacts Au–Ti–Pd–n^+-InP, formed by successive thermal deposition of metals in oil-free vacuum onto the n^+-n-n^{++}-n^{+++}-InP substrate heated to 300 °C have linear CVC within the temperature range 250…380 K. The temperature dependence ρ_c in this case is described by the thermal field emission mechanism. This fact distinguishes the contact Au–Ti–Pd–n^+-n-n^{++}-n^{+++}-InP from the ohmic contact Au–Ti–Ge–Pd–n^+-n-n^{++}-n^{+++}-InP, in which its advantage, associated with subdoping of the near-contact area of InP with germanium, offset by the structural heterogeneity of contact, causing linear increase in ρ_c with increasing the temperature.

References

1. H. Eisele, R. Kamua, Submillimeter–Wave InP Gunn Devices // *IEEE Trans. MTT*, **52**(10), p. 2371-2378 (2004).

2. H. Eisele, 480 GHz oscillator with an InP Gunn device // *Electron. Lett.* **46**(6), p. 422-423 (2010).

3. V. Papageorgiou, A. Khalid, C. Li, D.R.S. Cumming, Cofabrication of planar Gunn diode and HEMT on InP substrate // *IEEE Trans. Electron. Dev*. **61**(8), p. 2279-2784 (2014).

4. M.I. Maricar, A. Khalid, G. Dunn, D. Cumming, C.H. Oxley, Experimentally estimated dead space for GaAs and InP based planar Gunn diodes // *Semicond. Sci. Technol*. **30**, p. 012001-012005 (2015).

5. N. Braslau, J.B. Gunn, J.L. Staples, Metal-semiconductor contact for GaAs bulk effect devices // *Solid–State Electron*. **10**(5), p. 381-383 (1967).

6. P. Auray, A. Guivarc'h, H.L'Haridon, J.P. Mercier, Formation, microstructure et resistances des contacts Au-Ge/n-GaAs, Au-Ge/n-InP, Au-Zn/p-InP et Au-Be/p-InP // *Thin Solid Films*, **127**(1), p. 39-68 (1985).

7. R.T. Tung, The physics and chemistry of the Schottky barrier height // *J. Appl. Phys. Rev*. **1**, p. 011304-1-01130454 (2014).

8. T. Clausen, O. Leistiko, Metallurgical optimization for ohmic contacts to InP using conventional metallization schemes // *Microelectron. Eng.* **18**(4), p. 305-325 (1992).

9. M.A. Abraham, S-Y. Yu, W.H. Choi, R.T.P. Lee, S.E. Mohney, Very low resistance alloyed Ni-based ohmic contacts to InP-capped and uncapped $n^+In_{0.53}Ga_{0.47}As$ // *J. Appl. Phys*. **116**(16), p. 1645061-1645066 (2014).

10. Wu Degi, Ding Wuchang, Yang Shansham, Jia Rui, Jin Zhi, Liu Xinyi, Optimization of ohmic contact for InP-based transferred electronic devices // *J. Semiconductors*, **35**(3), p. 036001-036005 (2014).

11. P. Jian, D.G. Ivey, R. Bruce, G. Knight, Ohmic contact formation in palladium-based metallizations to n-type InP // *J. Electron. Mater.* **23**(9), p. 953-962 (1994).

12. P. Maltsev, Yu. Fedorov, R. Galiev, S. Mikhailovich, D. Gnatyuk, Millimeter range nitride devices // *Nanoindustry*, **3**(49), p. 40-51 (2014).

13. A. Dargys, J. Kundrotas, *Handbook on Physical Properties of Ge, Si, GaAs and InP*. Sci and Encyclopedia Publ., Vilnius, 1994.

14. S.J. Pearton, *Processing of Wide Band Gap Semiconductors: Growth, Processing and Applications*. Noyes Publ. Park Ridge. New Jersey, 2000.

15. A.V. Sachenko, A.E. Belyaev, N.S. Boltovets et al., Features of temperature dependence of contact resistivity in ohmic contacts on lapped n-Si // *J. Appl. Phys.* **112**(6), p. 063703-0637035 (2012).

16. V.P. Kladko, A.V. Kuchuk, P.M. Lytvyn et al., Substrate effects on the strain relaxation in GaN/AlN short-period superlattices // *Nanosc. Res. Lett.* **7**(1), p. 289-299 (2012).

17. S.M. Sze, Kwok K. Ng, *Physics of Semiconductor Devices*. 3rd ed. Wiley, New Jersey, 2007.

18. A.V. Sachenko, A.E. Belyaev, N.S. Boltovets et al., Mechanism of contact resistance formation in ohmic contacts with high dislocation density // *J. Appl. Phys.* **111**(8), p. 083701-083709 (2012).